Parameter dependences of the separatrix density in nitrogen seeded ASDEX Upgrade H-mode discharges

A. Kallenbach[1], H.J. Sun[1], D. Carralero[1], T. Eich[1], J. Hobirk[1], A. Scarabosio[1], M. Siccinio[1], ASDEX Upgrade team, EUROfusion MST1 team[2]

[1]*Max Planck Institute for Plasma Physics, D-85748 Garching, Germany,*

[2] *Meyer et al., Overview of progress in European Medium Sized Tokamaks towards an integrated plasma-edge/wall solution, accepted for publication in Nuclear Fusion*

Introduction

A very important interface parameter between core plasma performance and divertor power exhaust is the electron density at the separatrix. In a most simple and qualitative picture, a low separatrix density is beneficial for the plasma energy confinement [1] [2], while a high density enables and supports the achievement of divertor detachment [3]. An important tokamak operational limit, the H-mode density limit, is also connected to an upper limit of the separatrix density [4]. Direct measurements of the (upstream) separatrix density are not easily available due to uncertainties in the assignment of the separatrix position from equilibrium reconstruction. To overcome this problem, Thomson scattering is used which measures T_e and n_e at the same location, while the separatrix position is assigned via the power flux P_{sep} and an assumption for the width of the power carrying layer [5] [6] [7].

Experimental data base

A data base was set up of ASDEX Upgrade H-mode discharges from 2014-2016 with different deuterium gas puff and nitrogen seeding levels, plasma currents and separatrix crossing power, P_{sep} [8]. Time intervals of typically 0.5 s duration are considered, where D and N gas puff levels are sufficiently stationary and in balance with pumping. The separatrix position in the T_e profile is determined using a power width λ_q taken as 2/7 of the measured λ_{Te} according to Spitzer-Härm conduction [9] [7]. Figure 1 shows the line-averaged density and the subset with separatrix densities available of the data base versus the plasma current. With significant variations, both densities rise roughly proportional with the plasma current. The highest line-averaged densities approach the Greenwald density and are obtained under pronounced detachment conditions [8]. Figure 2 compares the Spitzer-Härm power decay length with the prediction of the Eich scaling [10] for nitrogen seeded discharges with different gas puff levels, heating powers,

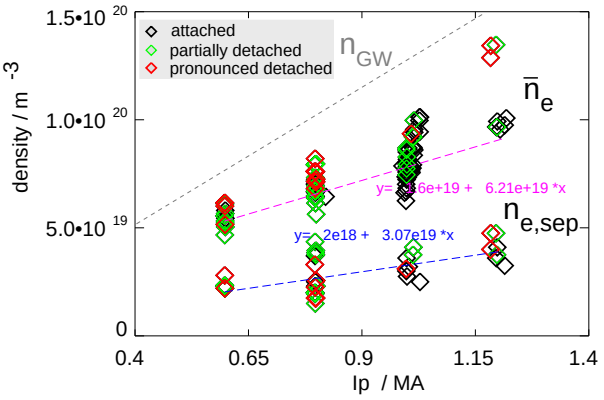

Figure 1: *Line-averaged and separatrix densities versus plasma current in the data base.*

plasma current etc. Due to the partly very high ELM frequencies and small ELM amplitudes, no effort was taken to cut out ELM effected time points from the Thomson scattering data, in contrast [9]. Good agreement is observed, albeit a trend towards higher values derived from Thomson scattering compared to the Eich prediction for higher plasma currents is clearly visible. This may be caused by the influence of the ELMs. Different parameter variations have been

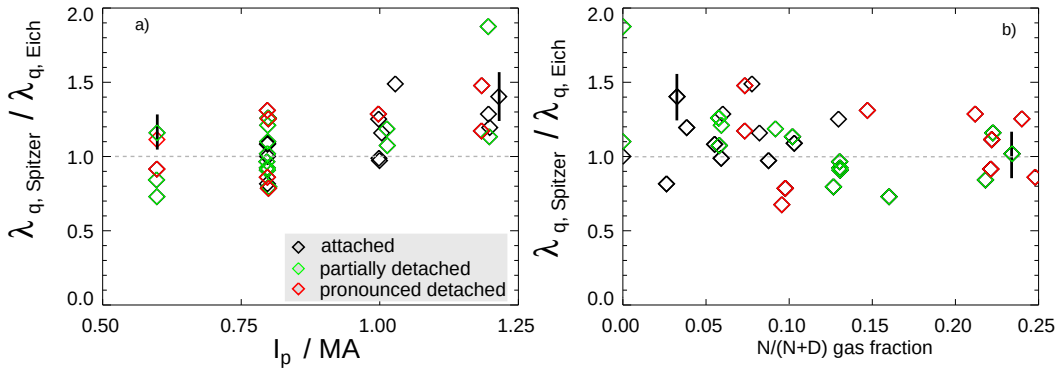

Figure 2: *a) Comparison of power decay lengths λ_q derived from Thomson scattering assuming Spitzer-Härm parallel electron heat conduction with the prediction of the Eich scaling for discharges with partially strong N and D puffing in the lower divertor and different degrees of detachment. Absolute values of the reference $\lambda_{q,Eich}$ vary from about 3.3 mm (0.6 MA) to 1.7 mm (1.2 MA) measured in radial direction in the omp. b) Deviation of $\lambda_{q,Spitzer}$ from the Eich scaling vs. nitrogen atomic fraction in the divertor gas.*

tested to identify a physics parameter responsible for the moderate deviation from the Eich scaling at high I_p. As shown in figure 2b, d= $\lambda_{q,Spitzer}$ / $\lambda_{q,Eich}$ shows no significant trend with nitrogen content or degree of detachment. The discharges shown here have acceptable or good H-mode confinement with $H_{98} \geq 0.8$ thanks to both N seeding and high heating power.

Various regression tests of the upstream separatrix density determined from Thomson scattering versus experimental parameters revealed the neutral divertor pressure, p_0, as leading parameter, see figure 3. There is an experimental trend of higher neutral pressure at higher currents, but this is believed to be produced by operational constraints like, e.g., the necessity to puff gas to avoid tungsten accumulation at higher plasma currrents or the better acceptance of a high p_0 at higher I_p. The scaling obtained, $n_{e,sep} = 2.7\ p_0^{0.31}$ (10^{19} m^{-3}, Pa), is also valid for the data subset at constant plasma current I_p= 0.8 MA. In a simple picture of tokamak gas balance, the divertor neutral pressure is proportional to the gas puff rate, with the effective pumping speed as a constant of proportionality. Thus p_0 can be regarded as engineering parameter. Figure 3b compares the measured neutral pressure with the gas puff rate, the expectation for pumping speeds between 25 and 30 m^3/s is indicated by a grey bar. In reality, the simple relation is modified by uptake or release of gas by the walls and a pressure dependence of the pumping speed. N seeding leads to a reduction of the pressure measured by the baratron, and also of $n_{e,sep}$ due to a change in the recycling pattern. This is explained by a high field side high density region [2].

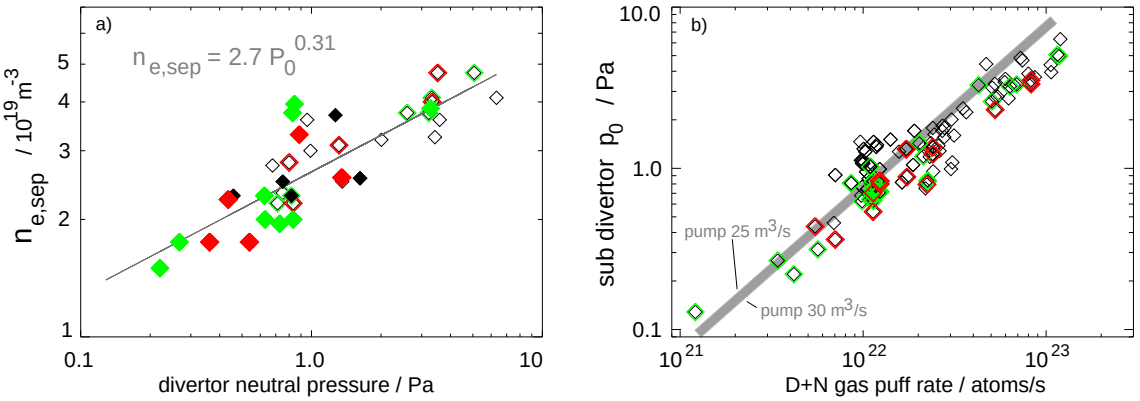

Figure 3: *a) Dependence of the upstream separatrix density on divertor pressure, measured by a baratron below the divertor. Full symbols denote data taken at I_p= 0.8 MA. b) Divertor pressure measured by a baratron below the roof baffle region vs. the sum of N an D gas puff rates. The grey line shows the expected pressure for an effective pumping speed of 25-30 m^3/s.*

Expectations from simple analytical considerations

In the following, the observed experimental trend between the upstream separatrix density n_{mid} and the neutral divertor pressure, p_0 is derived using simple 2-point model considerations [11], assuming dominant electron conduction and T_e=T_i [eV]. The plasma parameters in the divertor and midplane are closely coupled by pressure balance and heat conduction. Momentum losses and divertor radiation are considered via simple multiplier / loss factors f_{mom} and f_{rad} between outer midplane and sheath in front of the target:

$$f_{mom} = 2n_{div}T_{div}/(n_{mid}T_{mid}), \quad f_{rad} = 1 \; - \; bq_{\parallel,div}/q_{\parallel,mid} \tag{1}$$

A Mach=1 flow towards the target at the sheath is assumed, resulting in a reduction of the static pressure by a factor 2. We have also introduced a divertor heat flux broadening factor $b = \lambda_{int}/\lambda_q \approx 1 + 1.64S/\lambda_q$ with the exponential decay λ_q and the Gaussian broadening S [10]. The midplane temperature is approximated assuming Spitzer electron conductivity along the connection length L and the divertor heat flux is given by the sheath boundary condition:

$$eT_{mid} = e(\frac{7}{2\kappa})^{2/7} \; (Lq_{\parallel,mid})^{2/7}, \quad q_{\parallel,div} = \; \gamma(2/m_D)^{0.5} \; n_{div}(eT_{div})^{3/2}, \; \kappa = 2380\frac{W}{m \; eV^{7/2}} \tag{2}$$

The broadening b does not enter here since it is assumed to occur at low temperatures in the divertor. γ is the sheath energy transmission factor which is typically between 7 and 8, but can be as low as 5 for a tungsten surface when about 50 % of the ion energy is reflected. We want to establish a connection to the neutral pressure. For this we make the assumption that the neutral flux density measured in the sub-divertor equals the ion flux density perpendicular to the target averaged over the power channel width λ_{int}. This assumption turns out to be quite compatible with the experimental data.

$$\Gamma_0 = \; sin(\alpha) \; q_{\parallel,div}/(\gamma \; eT_{div}) = \; (1 - f_{rad}) \; sin(\alpha) \; q_{\parallel,mid} \; /(b \; \gamma \; eT_{div}) \tag{3}$$

α is the impact angle of the field line at the outer target, a typical value is 2.5^o. The radiative losses, which include the power loss due to charge exchange, are described by f_{rad}. Finally, by combination of eqns 1-3, we obtain for the upstream density

$$n_{mid} = \frac{2}{f_{mom}} (1 - f_{rad})^{1/2} \frac{1}{e} (\frac{2\kappa}{7L})^{2/7} (m_D/2)^{0.5} (b\ \gamma \sin(\alpha))^{-1/2} q_{\parallel,mid}^{3/14} \Gamma_0^{1/2} \quad (4)$$

Eq. 4 quite well reconciles the experimental finding for n_{mid} shown in figure 3. There is only a weak I_p dependence expected via $q_{\parallel,mid} \propto P_{sep}/\lambda_q$, $\lambda_q \propto 1/I_p$. The difference in the exponent for Γ_0 (0.5 vs. 0.3) may be explained by the impact of other coefficients like f_{mom}, f_{rad}, b and the weak $q_{\parallel,mid}^{3/14}$. A high divertor f_{rad} tends to reduce n_{mid}. The simple picture of balance of neutral fluxes to and from the divertor plasma may be impaired by geometrical effects and an imbalance of neutral sources and sinks in the inner and outer divertor.

Conclusions

Measurements of the upstream separatrix density for N seeded and unseeded H-modes reveal a strong correlation with the divertor neutral pressure, $n_{e,sep} \propto p_{0,div}^{0.3}$. Dependence on other experimental parameters appears to be weak. Due to particle balance, the divertor pressure can be regarded as engineering parameter being largely proportional to the gas puff rate. The relation of $n_{e,sep}$ and $p_{0,div}$ is reconciled by simple analytical considerations. Divertor optimization should envisage a high neutral flux at given upstream $n_{e,sep}$ for better power exhaust. Physics effects leading to broadening of the perpendicular heat flux width λ_{int} help to reduce $n_{e,sep}$.

Acknowledgements

This work has been carried out within the framework of the EUROfusion Consortium and has received funding from the Euratom research and training programme 2014-2018 under grant agreement number 633053. The views and opinions expressed herein do not necessarily reflect those of the European Commission.

References

[1] SCHWEINZER, J. et al., Journal of Nuclear Materials **266–269** (1999) 934.
[2] DUNNE, M. G. et al., Plasma Physics and Controlled Fusion **59** (2017) 014017.
[3] GOLDSTON, R. et al., Plasma Phys. Controlled Fusion (2017) 055015.
[4] BERNERT, M. et al., Plasma Physics and Controlled Fusion **57** (2015) 014038.
[5] NEUHAUSER, J. et al., Plasma Physics and Controlled Fusion **44** (2002) 855.
[6] STANGEBY, P. C. et al., Nucl. Fusion **55** (2015) 093014.
[7] SUN, H. et al., submitted to Plasma Physics and Controled Fusion (2017).
[8] KALLENBACH, A. et al., Nuclear Fusion **55** (2015) 053026.
[9] SUN, H. J. et al., Plasma Physics and Controlled Fusion **57** (2015) 125011.
[10] EICH, T. et al., Phys. Rev. Lett. **107** (2011) 215001.
[11] STANGEBY, P., *The Plasma Boundary of Magnetic Fusion Devices*, Institute of Physics Publishing, Bristol and Philadelphia, 2000.